

Article

Effect of Saturation Degree on Mechanical Behaviors of Shallow Unsaturated Expansive Soils

Jinpeng Li ^{1,2}, Hong Xu ^{1,3,*}, Lichuan Chen ^{1,3,*}, Boyi Li ^{1,3}, Dan Liang ^{1,3}, Shicong Ren ¹, Shilei Zhang ⁴ and Jun Wang ²

¹ Technology Innovation Center of Geohazards Automatic Monitoring, Ministry of Natural Resources, Chongqing Engineering Research Center of Automatic Monitoring for Geological Hazards, Chongqing 401120, China

² School of Urban Railway Transportation, Shanghai University of Engineering Science, Shanghai 201620, China

³ School of Civil Engineering, Chongqing University, Chongqing 400044, China

⁴ Shenzhen Metro Construction Group Co., Ltd., Shenzhen 518026, China

* Correspondence: xuhong_cqdy@163.com (H.X.); chenlichuandy@163.com (L.C.)

Abstract: In the southwest of China, there are widely distributed expansive soils. However, to save costs and manage the speed of construction, these shallow expansive soils are often filled with subgrade materials. Therefore, it is necessary to clearly understand the mechanical behaviors of unmodified shallow expansive soils. Current research on the mechanical behaviors of shallow expansive soils is mainly focused on shear and compressive strengths but rarely on the tensile strength since general tests are costly, time consuming, and difficult to conduct. Therefore, uniaxial tensile, unconfined compression and direct shear tests were carried out to study the mechanical behavior of shallow unsaturated expansive soils under different saturation degrees, and the tests analyzed the change mechanism of its mechanical behavior. The following were found: (1) with an increase in saturation degree, the uniaxial tensile strength, unconfined compressive strength, shear strength, cohesive force, and internal friction angle first increased and then decreased; (2) when the saturation degree increased from 18.7% to the saturation degree corresponding to the peak, the uniaxial tensile strength, unconfined compressive strength, cohesive force, and internal friction angle increased by about 11 times, 3.24 times, 2.34 times, and 0.52 times, respectively; (3) when the saturation degree increased from the saturation degree corresponding to the peak to 80.3%, they decreases by about 42%, 51.4%, 36%, and 50%, respectively; (4) with the increase in dry density, the saturation degree corresponding to the peak of uniaxial tensile strength gradually increased, while the saturation degree corresponding to the peak of unconfined compressive and shear strength did not significantly change.

Keywords: expansive soils; saturation degree; tensile strength; compressive strength; shear strength



Citation: Li, J.; Xu, H.; Chen, L.; Li, B.; Liang, D.; Ren, S.; Zhang, S.; Wang, J. Effect of Saturation Degree on Mechanical Behaviors of Shallow Unsaturated Expansive Soils. *Sustainability* **2022**, *14*, 14617. <https://doi.org/10.3390/su142114617>

Academic Editors: Kai Wang, Yubing Liu and Xiaojun Feng

Received: 27 September 2022

Accepted: 3 November 2022

Published: 7 November 2022

Publisher's Note: MDPI stays neutral with regard to jurisdictional claims in published maps and institutional affiliations.



Copyright: © 2022 by the authors. Licensee MDPI, Basel, Switzerland. This article is an open access article distributed under the terms and conditions of the Creative Commons Attribution (CC BY) license (<https://creativecommons.org/licenses/by/4.0/>).

1. Introduction

In unsaturated expansive soil regions, ground upheaval has caused a serious threat to the safety of building structures. The use of on-site expansive soils as a foundation backfill materials is one of the main solutions to reduce or eliminate ground movement, with good economic, social, and environmental benefits. However, researchers need to have a clear understanding of the mechanical behaviors of expansive soils before using them as a basic building material. Therefore, many scholars have conducted extensive research on the mechanical behaviors of expansive soils.

The bearing capacity of foundations [1], retaining wall earth pressure, and slope stability [2–4] in engineering are all directly related to the shear strength of soils, and the shear strength of expansive soils is easy to obtain with simple straight shear tests. The shear strength of expansive soils has become a popular research topic in recent years. Many researchers have systematically carried out experimental studies on the effects of many factors on the shear strength of expansive soils by changing test conditions and

methods, such as the effects of water content and dry density [5–10]; cyclic wetting and drying [6,11–13]; temperature [14]; freeze–thaw cycle [15]; sodium chloride solution [16] on the shear strength of expansive soils; and the relationship between crack rate and shear strength [17–19]. Meanwhile, Zhai et al. (2019, 2020a) studied the relationship between the soil–water characteristic curve and the shear strength of unsaturated soil, and they predicted shear strength based on their relationship [20,21].

In engineering applications, the expansion and contraction characteristics of expansive soils must be weakened by modification techniques to meet the needs of the project; therefore, research on the compressive strength of expansive soils is mainly focused on modified expansive soils. Based on the existing modification technology, the existing study on the compressive strength of expansive soils can be roughly divided into three types: (1) inorganic binder modification technology, (2) chemical reagent and bio-enzyme modification technology, and (3) physical modification technology. The main inorganic binding for the modification of expansive soils is lime, cement, and marble. Some scholars have used this inorganic binder to improve the compressive strength of expansive soils [22–27]. Chemical reagent and bio-enzyme modification techniques refer to the practice of modifying expansive soils using biological enzymes or chemical reagents [28–31]. Soltani et al. (2019) investigated the effect of compressive strength on treating expansive soils with the chemical reagent of sulphonated oil agents [32]. Liu et al. (2009) used ionic curing agents to modify expansive soils and found that as the compression coefficient of expansive soil decreased, the compression modulus increased, and the compressive strength of soil was significantly increased overall [33]. Some scholars also used physical modification technology to improve the compressive strength of expansive soils, mainly including fiber-reinforced modifications [34–36] and scrap tires pellet modification [37]. However, the expansive soils are non-modified in their natural state.

In fact, the tensile strength of soils is low and unstable, which results in insufficient research, which is usually not considered for tensile strength. Meanwhile, the tensile strength of expansive soils is mainly obtained by tests, but tests of the tensile strength of expansive soils is generally costly, time consuming, and difficult to conduct. Therefore, there are few studies on the tensile strength of expansive soils in the literature. The study of Nitin et al. (2021a) found that the tensile strength of expansive soils would increase when the CF fiber increased the interfacial interaction of soil particles [38]. Arvind et al. (2007) discussed the influence of fly ash, lime, and polyester fibers on the tensile strength of expansive soils [39]. Rabab'ah et al. (2021) found that the inclusion of glass fibers in expansive soils would make the indirect tensile strength of expansive soils first increase and then decrease with the glass fiber [33]. Nitin et al. (2021b) found that the tensile strength of expansive soils treated with the bio-stimulation MICP treatment significantly improved because calcite content precipitation increases the interfacial interaction between soil particles [40]. Sun et al. (2003, 2004, 2007) carried out a triaxial tensile test on unsaturated clay soils compacted at different initial dry densities and found that the tensile strength of the soils is one of the most important factors in determining the collapse deformation of clay [41–43]. Zhai et al. (2020b) predicted the tensile strength of sandy soil using the soil–water characteristic curve [44]. However, the tensile strength of shallow unsaturated expansive soils must be investigated under certain conditions, such as the wet and dry circulation of expansive soils, the lifting and hauling of expansive soils blocks, and the generation slip of expansive soil slopes. These situations will inevitably generate tensile stress, leading to expansive soil damage.

According to the above discussion, the current research on the strength of unmodified shallow expansive soils mainly focuses on shear strength, while studies on tensile strength and compressive strength are lacking. However, during practical engineering, the stress state of the expansive soils is connected with the tensile stress, compressive stress, and shear stress, and the damage to expansive soils is simultaneously affected by tensile strength, compressive strength, and shear strength. Since expansive soils expand after absorbing water and shrink after losing water, it is necessary to study the change in mechanical

behaviors in shallow unsaturated expansive soils from the perspective of their degree of saturation. Based on the shortcomings of current research, tensile–compressive–shear strength tests of shallow unsaturated expansive soils were carried out to investigate the effect of saturation degree on the mechanical behaviors of shallow unsaturated expansive soils, as described in this paper. Meanwhile, the change mechanism of mechanical behaviors of shallow expansive soils is analyzed.

2. Materials and Methods

2.1. Materials

2.1.1. Testing Soils

The expansive soils used for the present investigation were sampled from a depth of about 2–3 m in Xiashi Town, Chongzuo City, Guangxi Province, China. The natural moisture content of expansive soil is 32.5%, the optimum moisture content is 24%, and the natural dry density is 1.40 g/cm³. The particle size distribution curve and the other basic soil parameters for expansive soils are shown in Figure 1 and Table 1, respectively. The soils are classified as clay with weak expansibility according to the Chinese standard for technical code for buildings in expansive soil regions (GB 50112-2013). According to the plasticity chart (see Figure 2) of the Chinese Ministry of Water Resources (2019) and a related study by Wang et al. (2020) [45], the sample is a high-liquid limited clay.

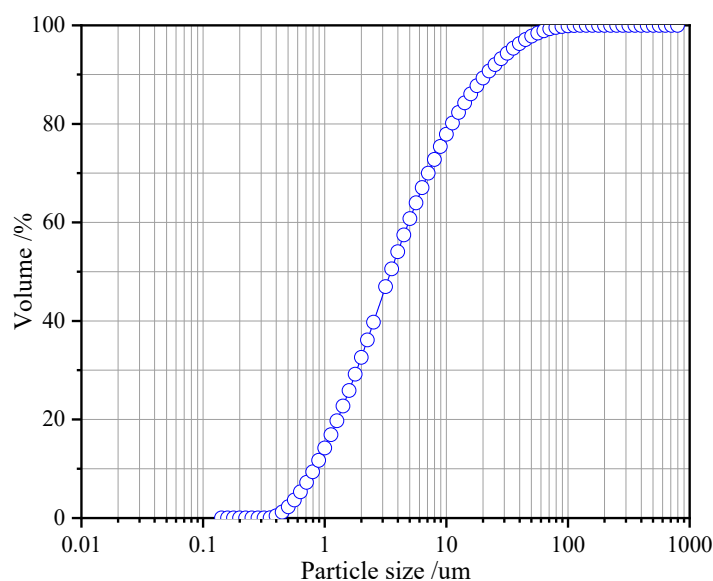


Figure 1. Particle size distribution curve for expansive soils.

Table 1. The basic parameters of expansive soils.

Specific Gravity	Liquid Limit /%	Plastic Limit /%	Plasticity Index	Free Expansion Rate /%
2.80	59.11	24.68	34.43	42.8

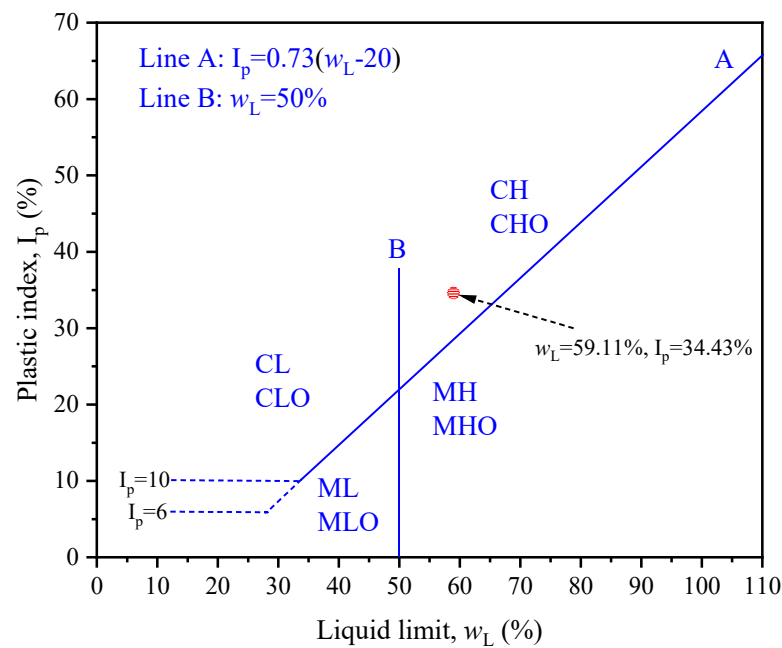


Figure 2. Plasticity chart for fine-grained soil classification.

2.1.2. Preparation of Specimens

This paper uses a new method to prepare wet soils with initial moisture contents of 7%, 13%, 17%, 21%, 23%, 26%, and 31%. The dry density of soil samples was maintained at 1.30, 1.35, and 1.40 g/cm³ by a weighing method. The preparation of the compacted specimens was performed using the static compaction method, and the compaction conditions were the same. The soil specimens for the uniaxial tensile test and the unconfined compressive test were cylinders with a diameter of 38 mm and a height of 76 mm, and the soil specimens for the direct shear test were cylinders with a diameter of 61.8 mm and a height of 20 mm. Compared with the traditional method of preparing wet soils, this new method can prepare more wet soils during the same time, as shown in Figure 3. The preparation process is as follows:

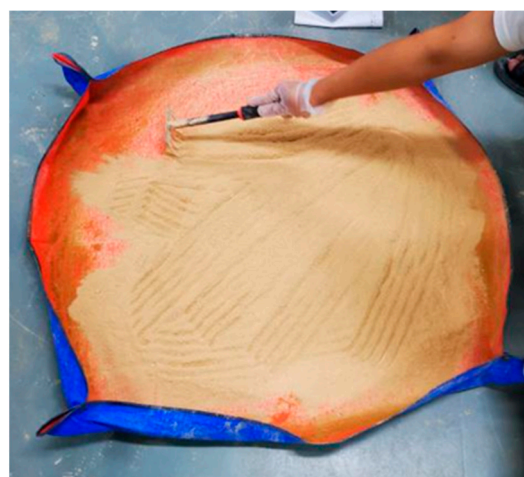


Figure 3. The wet soils were prepared.

(1) The expansive blocks of soil were crushed with a rubber hammer, passed through a 2.0 mm sieve, and dried in an oven. (2) The dried and sieved expansive soils were weighed using scales based on the requirements for the tests. (3) The sampled soils were tiled on the test tarp. (4) The water mist was sprayed on the dried soils using a spray bottle until the

soil surface was thoroughly wet. (5) These soils were stirred with a rake to ensure the even mixing of water and soil particles; then, recently added water and soil were stirred until the soil reached the target water content. (6) The mixed soils were placed in a sealed black plastic bag for 48 h to balance the water of the soils in a plastic bag. Figure 4 is a flow chart showing the preparation of wet soils.

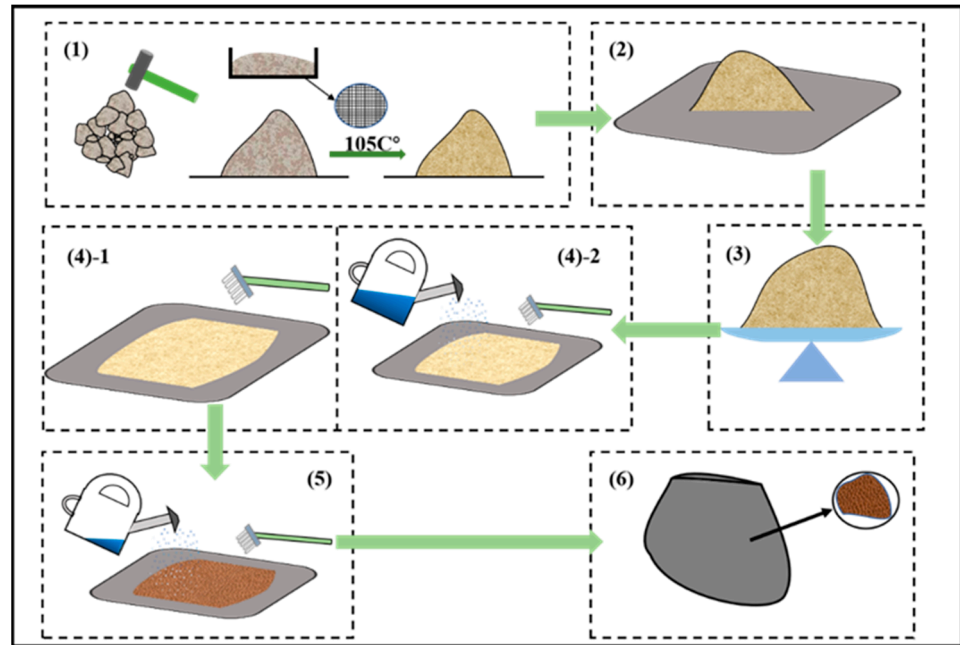


Figure 4. The flow chart for preparing wet soils.

The shear specimen and uniaxial tensile specimen were prepared using two molds (see Figures 5 and 6).

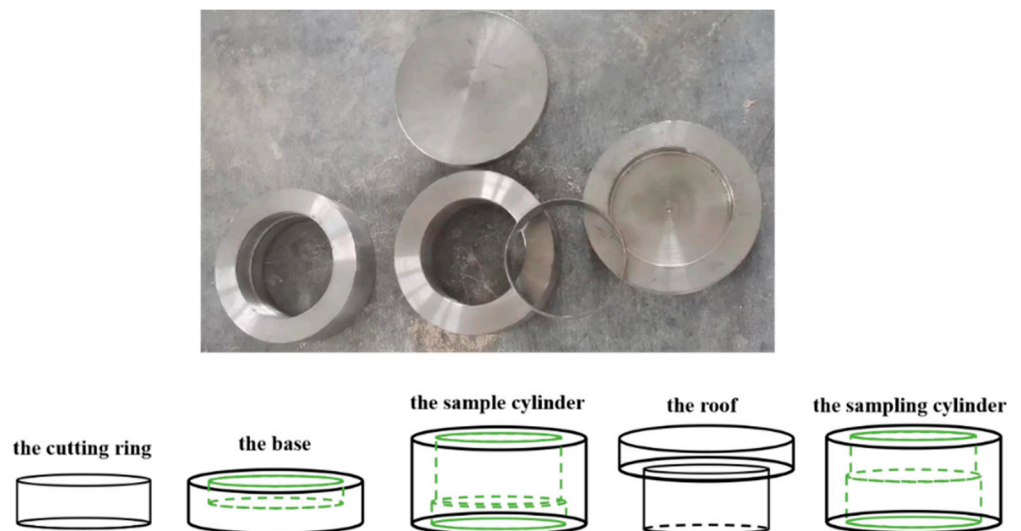


Figure 5. The mold for preparing the shear specimen.

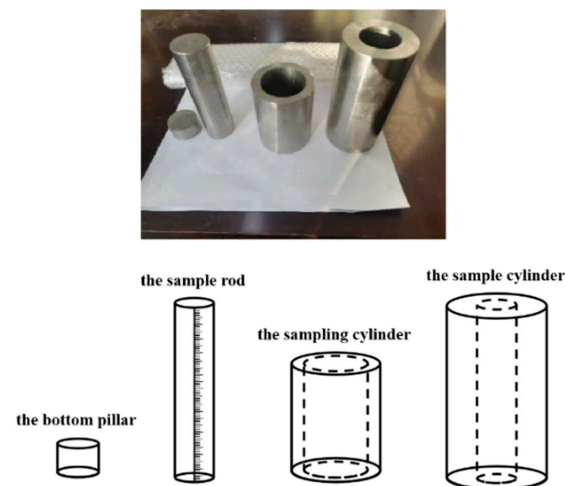


Figure 6. The mold for preparing the uniaxial tensile specimen.

The preparation-specific steps for shear specimens are as follows:

(1) Vaseline was painted on the inner wall of the cutting ring. (2) The cutting ring was placed on the base of the mold, and then the sample cylinder of the mold was nested on the cutting ring. (3) The required wet soil was taken away according to the size of the cutting ring (diameter 61.8 mm, height 20 mm). (4) The sampled wet soil was poured into the mold, and the wet soil surface was smoothed. (5) The roof of the mold was placed on the sample cylinder. (6) The hydraulic system was used to exert pressure on both ends of the mold. (7) The prepared sample was taken out from the cutting ring by the sampling cylinder. The direct shear specimen was obtained following the above steps: (1) to (7) (Figure 7).

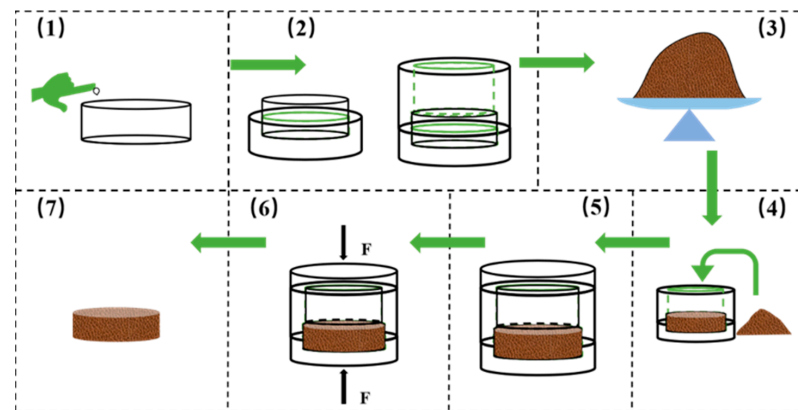


Figure 7. The preparation flow chart of the shear specimen.

The preparation-specific steps for uniaxial tensile specimen are as follows:

(1) Vaseline was painted on the inner wall of the sample cylinder. (2) The bottom pillar was embedded in the sample cylinder. (3) The required wet soil was taken away according to the size of the tensile sample (diameter 38 mm, height 76 mm). (4) The sampled wet soil (about 1/3) was poured into the mold, and the wet soil surface was smoothed. (5) The sample rod was put into the sample cylinder. (6) The hydraulic system was used to exert pressure on both ends of the mold, and the degree of sample compaction was controlled by the scale marked on the sample rod. (7) The sample rod was removed from the sample cylinder, and then the sample surface was shaved. (8) Steps (4) to (7) were repeated twice. (9) The prepared sample was taken out from the sample cylinder by the sampling cylinder. The uniaxial tensile specimen was obtained after following steps (1) to (9) (Figure 8).

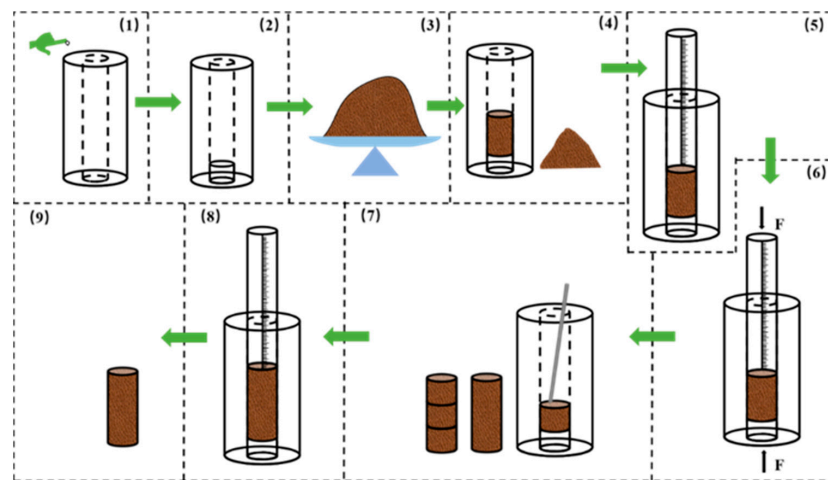


Figure 8. The preparation flow chart of the uniaxial tensile specimen.

2.2. Test Methods

2.2.1. Uniaxial Tensile and Unconfined Compression Tests

In the uniaxial tensile test and unconfined compression test, a new type of apparatus was applied. This apparatus is an improvement of the triaxial test device, which is shown in Figure 9. The processes of the uniaxial tensile and unconfined compression tests are as follows: (I) Samples (5) and (8) were glued at each end of (6) using a fast-setting glue. In the uniaxial tensile test, (8) needed to be fixed onto (9) by (7) to ensure (6) was tensile. (II) Sample (4) was adjusted, and the test parameters were set. (III) Sample (6) was stretched (or compressed) at a constant speed of 0.4 mm/min by setting the parameters of (10). (IV) The tensile (or compressive) force was measured by (4) during the tensile (or compressive) process and transmitted to the data acquisition equipment (11) in real time. The tensile strain can be obtained according to the mathematical relationship between the stretching (or compression) speed and time. (V) When the observed tensile (or compressive) force value sharply decreased and significant cracks were observed in (6), it was concluded that (6) was damaged, and the test ended.

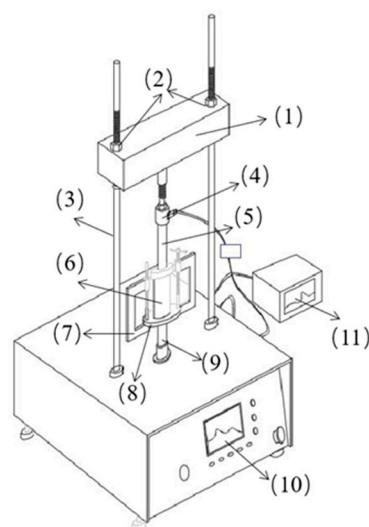


Figure 9. Uniaxial tensile and unconfined compression test apparatus: (1) beam, (2) two nuts, (3) loading frame, (4) pressure transducer, (5) loading rod, (6) soil sample, (7) metal clamps, (8) carrier plate, (9) lifting table, (10) control panel, and (11) transmitter.

2.2.2. Direct Shear Test

During practical engineering, the vertical pressure of shallow unsaturated expansive soils is generally less than 50 kPa. Therefore, the vertical pressure of the specimen was maintained at values of 6.25 kPa, 12.5 kPa, 25 kPa, and 50 kPa during the shearing process. In this study, the conventional strain-controlled direct shear equipment was used for the direct shear test. The process of the direct shear test is as follows:

(1) The different water content and dry density of the samples were loaded into the direct shear tester. (2) The low normal stresses of 6.25 kPa, 12.5 kPa, 25 kPa, and 50 kPa were applied to the specimen by hanging different weights on the lever. (3) The specimen was sheared at a shear rate of 0.2 mm/min. (4) A constant reading in the transmitter recording data indicated that the shear test was complete.

For a given soil, G_s always remains constant, and both w and e may vary under different states [46]. Therefore, the w and e in different states should first be determined to obtain the saturation degree of soil. The water content and the void ratio of soil samples at a particular moment in time can be obtained by Equations (1) and (2):

$$w = \frac{(m_0 - m_d)}{m_d} \times 100\% \quad (1)$$

$$e = \frac{G_s \times (1 + w)\rho_w}{\rho} - 1 \quad (2)$$

where the saturation degree can be obtained by Equation (3):

$$S_r = \frac{G_s \times w \times 100\%}{e} \quad (3)$$

where w is the water content, e is the void ratio, G_s is the specific gravity, ρ is the natural density, ρ_w is the density of water, m_0 is the mass of specimens at a particular time, and m_d is the mass of dried soil. From this, the saturation degree of specimens at different water contents and dry densities, as well as the curve variation laws of tensile, compressive, and shear strength of specimens at different saturation degrees can be obtained (see Chapter 3). When the dry density of specimens was 1.30 g/cm³, the pore water of specimens gradually increased with the increase in water content, so that the saturation degree increased, as shown in Figure 10. Because the size of specimens was equal, the dry density of specimens increased from 1.30 g/cm³ to 1.40 g/cm³, and their internal pores were compressed, resulting in a reduction in pore volume. Therefore, when the same water content is maintained, the saturation degree of specimens increases as the dry density increases, as shown in Figure 10.

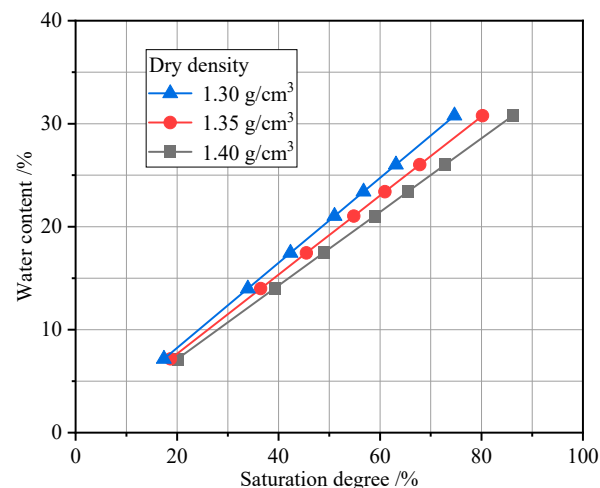


Figure 10. Relationship between saturation degree vs. water content.

3. Test Results

3.1. Effect of Saturation Degree on Uniaxial Tensile Strength of Specimens

The uniaxial tensile strength of shallow unsaturated expansive soils first increased and then decreased with the increase in saturation degree (see Figure 11). The initial saturation degree of specimens under different dry densities was about 18.7% (average), the saturation degree corresponding to the peak uniaxial tensile strength was about 57.1% (average), and the end saturation degree was about 80.3% (average). From an 18.7% saturation degree to 57.1% saturation degree, the uniaxial tensile strength of the specimens gradually increased. Compared with the initial state, the uniaxial tensile strength of the specimens increased by about 11 times. From a 57.1% saturation degree to 80.3% saturation degree, the uniaxial tensile strength of the specimens decreased by about 42%. When the dry density increased from 1.30 g/cm^3 to 1.40 g/cm^3 , the saturation degree corresponding to the peak uniaxial tensile strength of the specimens gradually increased (see Figure 11). When the dry density increased by 0.1 g/cm^3 (from 1.30 g/cm^3 to 1.40 g/cm^3), the saturation degree corresponding to the uniaxial tensile strength peak increased by about 28%. When the saturation degree of the specimens was less than 50%, the change in dry density had little effect on the uniaxial tensile strength of the specimens. However, when the saturation degree of the specimens was greater than 50%, the uniaxial tensile strength of the specimens with different dry densities greatly varied (see Figure 11). With the increase in saturation degree, the difference in the water content of the specimens with different dry densities (the saturation degree was the same) was gradually significant, which is the reason for this phenomenon (see Figure 10). When the saturation degree was the same (less than 50%), the difference in the water content between different dry densities was small. However, when the saturation degree was the same (saturation degree greater than 50%), the water content between different dry densities greatly varied. Therefore, this phenomenon also shows that water content is an important reason for the change in uniaxial tensile strength.

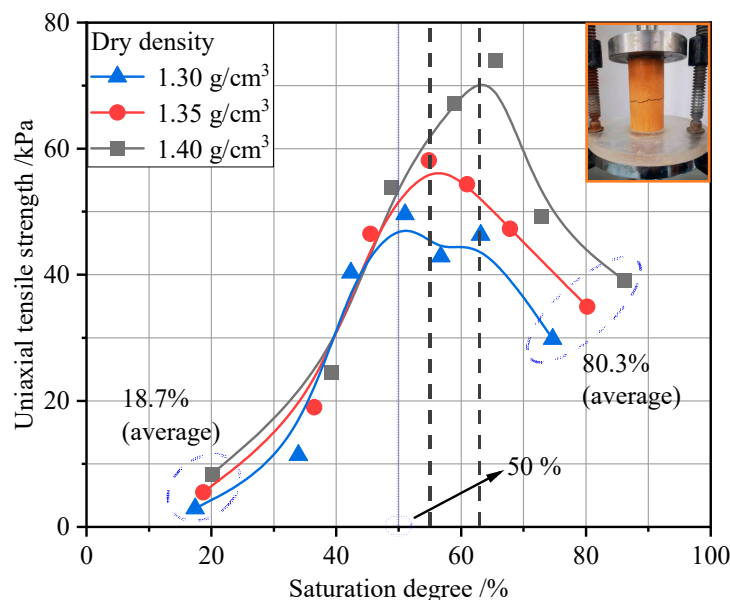


Figure 11. Effect of saturation degree on uniaxial tensile strength of specimens.

3.2. Effect of Saturation Degree on Unconfined Compressive Strength of Specimens

The unconfined compressive strength of shallow unsaturated expansive soils first increased and then decreased with the increase in saturation degree, and this changing trend was similar to the changing trend in uniaxial tensile strength. The difference is that the change in dry density had little effect on the saturation degree corresponding to the peak unconfined compressive strength of the specimens, and the saturation degree corresponding to the peak was about 50% (see Figure 12). A 50% saturation degree could

be used as the demarcation point of its increase or decrease. From the initial state to a 50% saturation degree, the unconfined compressive strength of the specimens under different dry densities was about 4.24 times that of the initial state. When the saturation degree reached 50%, the unconfined compressive strength of the specimens was close to the peak (see Figure 12). From a 50% saturation degree to an 80.3% saturation degree, the unconfined compressive strength attenuation was about 55%. When the saturation degree was 50%, the dry density changed from 1.40 g/cm^3 to 1.30 g/cm^3 , and the peak unconfined compressive strength attenuation was about 51.4%.

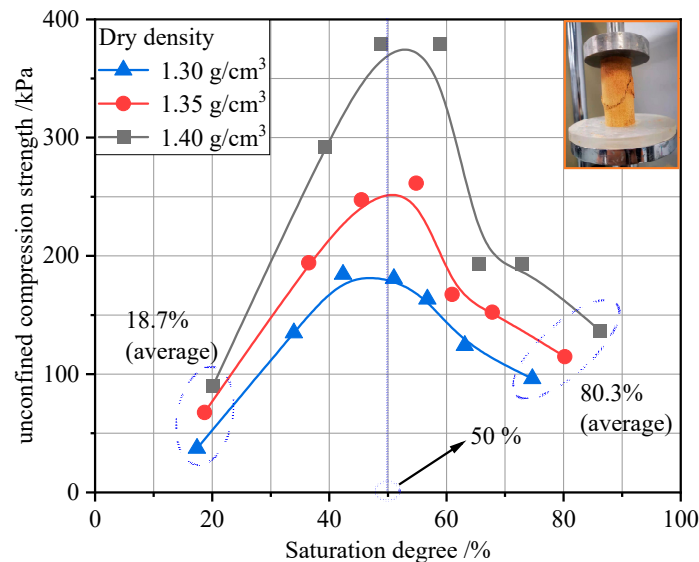


Figure 12. Effect of saturation degree on unconfined compressive strength of specimens.

3.3. Effect of Saturation Degree on Shear Strength of Specimens

The shear strength of the shallow unsaturated expansive soils also first increased and then decreased with the increase in saturation degree, and its change trend was similar to that of unconfined compressive strength. Under different vertical pressures and dry densities, the saturation degree corresponding to the peak shear strength of the specimens was about 50%. From the initial state to a 50% saturation degree, the shear strength of the specimens gradually increased. With the further increase in saturation degree, the shear strength of the specimens gradually decreased (see Figure 13a–d). When the vertical pressure was 6.25 kPa, from a 18.7% saturation degree to a 50% saturation degree, the shear strength of the specimens increased by about 1.8 times compared with the initial state. From a 50% saturation degree to an 80.3% saturation degree, the shear strength of the specimens was attenuated by about 37%. When the saturation degree and dry density were the same, the shear strength of the specimens gradually increased with the increase in vertical pressure (see Figure 13a–d). Meanwhile, when the vertical pressure and saturation degree were the same, the shear strength of the specimens increased with the increase in dry density (see Figure 13a–d).

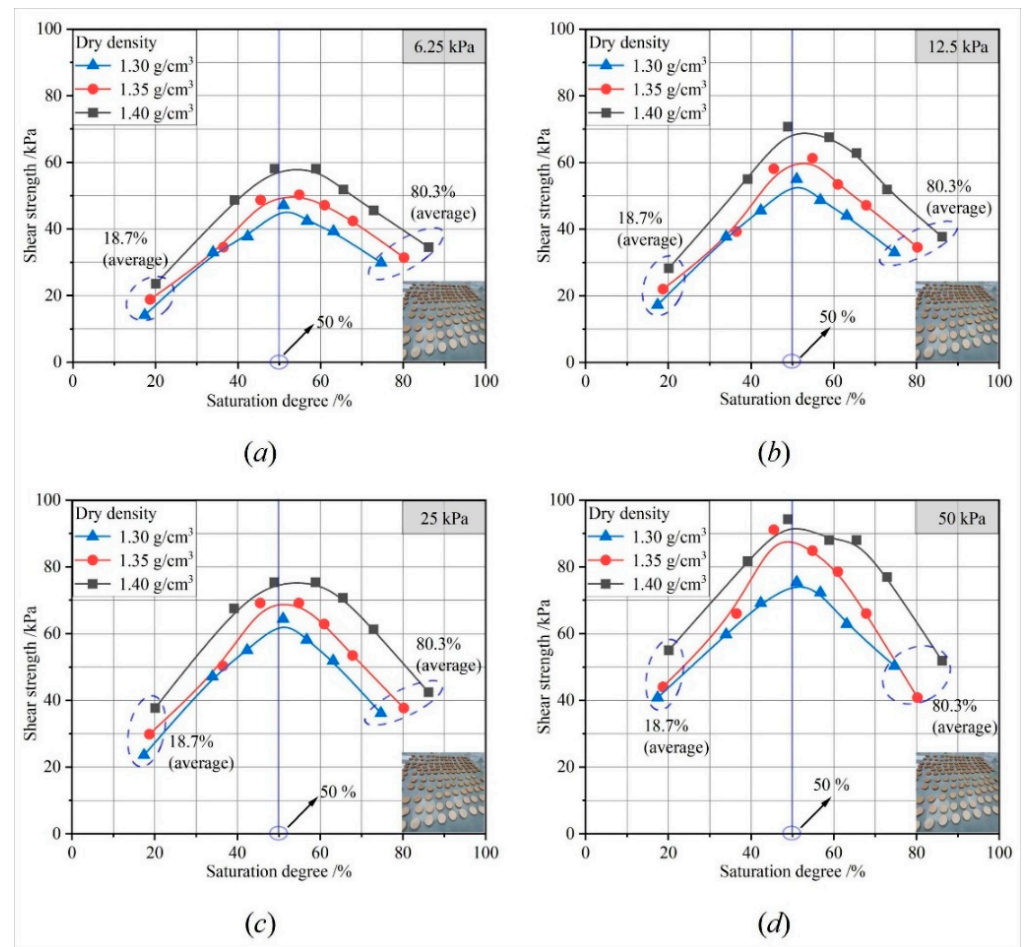


Figure 13. Effect of saturation degree on shear strength of specimens: (a), (b), (c), and (d) are under vertical pressure of 6.25, 12.5, 25, and 50 kPa, respectively.

Shear strength parameters include cohesive force and internal friction angle. With the increase in the saturation degree, the cohesive force and internal friction angle also first increased and then decreased (see Figure 14a,b). Compared with the change trend in the shear strength of the expansive soils with water content, the change trend in the shear strength parameters of coral gravelly sand with water content was different [47,48]. With the increase in water content, the internal friction angle first increased and then decreased. However, the cohesive force increases with increasing water content [47]. Capillary cohesive force is the main reason for the difference in the coral gravelly sand cohesive force. The change range in the water content of coral gravelly sand in the study was small, and the capillary pressure increased with the increase in water content. Therefore, the cohesive force of coral gravelly sand increased with the increase in water content. The saturation degree corresponding to the peak cohesive force and internal friction angle of the specimens was about 50%. When the saturation degree was less than 50%, the cohesive force and internal friction angle of the specimens increased with the increase in saturation degree. When the saturation degree was greater than 50%, the cohesive force and internal friction angle decreased with the increase in saturation degree. From an 18.7% saturation degree to 50% saturation degree, the cohesive force and internal friction angle increased by 2.34 times and 0.52 times, respectively. From a 50% saturation degree to an 80.3% saturation degree, the cohesive force and internal friction angle decreased by 36% and 50%, respectively. When the saturation degree was the same, the cohesive force increased with the increase in dry density (see Figure 14a). However, the dry density had little effect on the internal friction

angle of the specimens (see Figure 14b). When the dry density was between 1.40 g/cm^3 and 1.30 g/cm^3 , the peak cohesive force decreased by 25.7%.

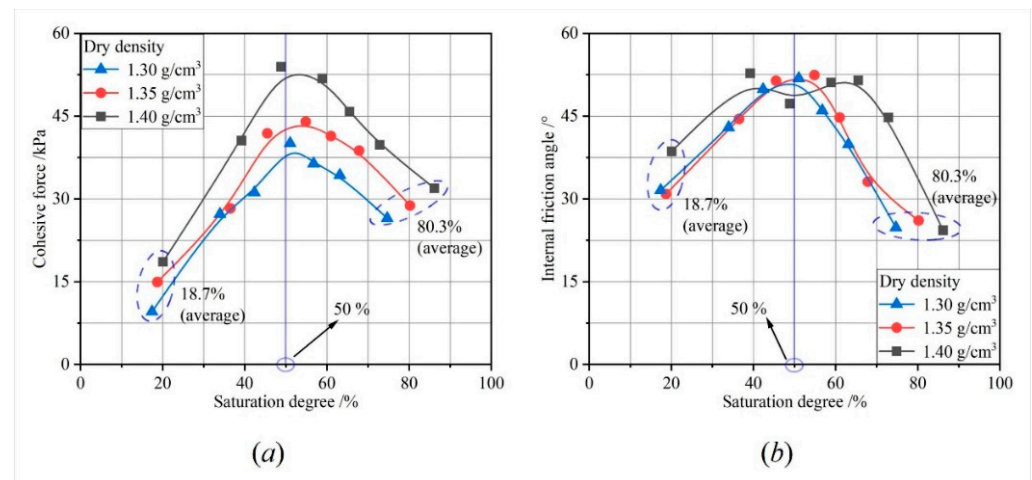


Figure 14. Effect of saturation degree on shear strength parameters: (a) effect of saturation degree on cohesive force c ; (b) effect of saturation degree on internal friction angle φ .

4. Mechanism Analysis

4.1. Mechanistic Analysis of Changes in Uniaxial Tensile Strength of Specimens

The microstructure of expansive soils is complex. In this regard, SEM tests were carried out to observe the microstructure of the expansive soils and the mechanism analysis (see Figure 15). There were three main reasons for the change in uniaxial tensile strength. (1) At the beginning of the test, the initial saturation degree of specimens was about 18.7%, and the pores were mainly in a dry and unsaturated state. When the saturation degree was 18.7% and gradually increased to the saturation degree corresponding to the peak tensile strength, the pores in the dry state became unsaturated. Since the pores in the unsaturated state produce capillary pressure [49], the uniaxial tensile strength increased. When the saturation degree of specimens gradually increased to 80.3%, the pores in the unsaturated state became saturated or nearly saturated. The capillary pressure generated by the pores gradually decreased and disappeared, and the uniaxial tensile strength decreased. The capillary pressure mechanism is shown in Figure 16. (2) There was a good linear relationship between saturation and water content (see Figure 10). The expansive soils contained a large number of hydrophilic mineral components [50,51] that could react with water molecules to form soluble colloids. The saturation degree was 18.7% at the beginning of the test, and the water content of the specimens was low. Therefore, the specimens contained many hydrophilic mineral components that had not been completely hydrated, and the soluble colloid content produced by hydration was lower. When the saturation degree was 18.7%, the water content of the specimens gradually increased to the saturation degree corresponding to the peak tensile strength. The hydrophilic mineral components in the specimens completely hydrated in a gradual process. During this process, the content of the soluble colloids produced by hydration gradually increased and reached a peak. Since soluble colloids strengthen the connection between soil particles [52,53], uniaxial tensile strength also increased (see Figure 11). The hydration mechanism of the hydrophilic mineral components in expansive soils is shown in Figure 17. When the saturation degree corresponding to the peak tensile strength gradually increased to 80.3%, the soluble colloids gradually began to dissolve. Therefore, the uniaxial tensile strength gradually decreased (see Figure 11). (3) When the saturation degree of the specimens was the same, the number of soil particles per unit of volume increased with the increase in dry density (the size and preparation method of the specimens were the same) [54]. This made the structure of

the specimens more stable and resistant to external forces. Therefore, the uniaxial tensile strength gradually increased.

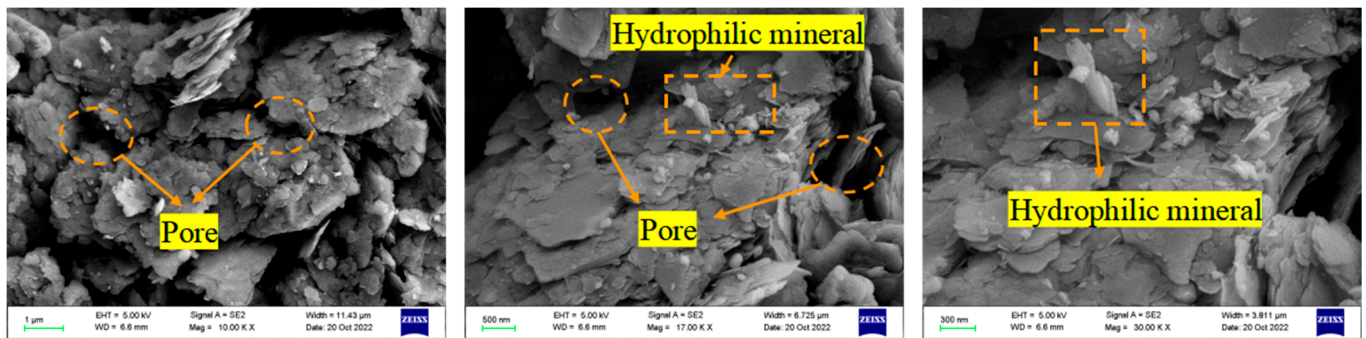


Figure 15. The SEM testing of expansive soils.

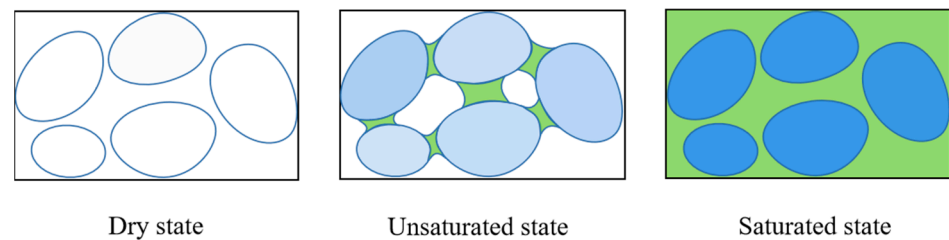


Figure 16. The capillary pressure mechanism.

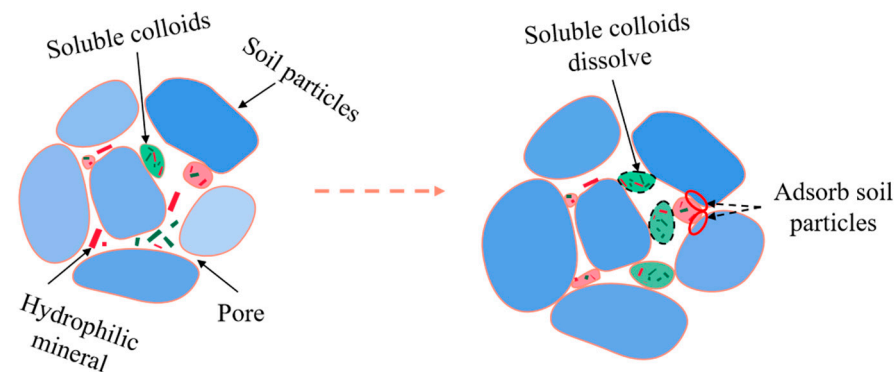


Figure 17. The hydration mechanism of hydrophilic mineral components.

4.2. Mechanistic Analysis of Changes in Unconfined Compressive Strength of Specimens

There were also three main reasons for the change in the unconfined compressive strength. (1) Expansive soils will expand after absorbing water and shrink after losing water [55]. With the increase in saturation degree, the soil particles expanded and deformed, and the cumulative pore volume continuously decreased (see Figure 18). When the saturation degree was low, the soil particles absorbed water and expanded, resulting in an expansion force to offset part of the pressure. Therefore, the unconfined compressive strength of the specimens increased. When the saturation degree was high, the soil particles expanded and were destroyed, and the expansion force gradually decreased and disappeared. Therefore, the unconfined compressive strength of the specimens was reduced. The mechanisms of soil particles and pore changes are shown in Figure 19. (2) According to the analysis of the uniaxial tensile strength mechanism, with the increase in saturation degree, the content of the soluble colloid produced by the hydration of hydrophilic mineral components first increased and then decreased. Due to the existence of colloids, the connection between soil particles can be strengthened [52], which makes the structure of

the specimens more stable. Therefore, the unconfined compressive strength first increased and then decreased with the increase in the saturation degree. (3) When the saturation degree of the specimens was the same, with the increase in dry density, the soil particles were arranged much closer. Therefore, the specimen structure was more stable, and the unconfined compressive strength was higher (similar to the effect of dry density on uniaxial tensile strength).

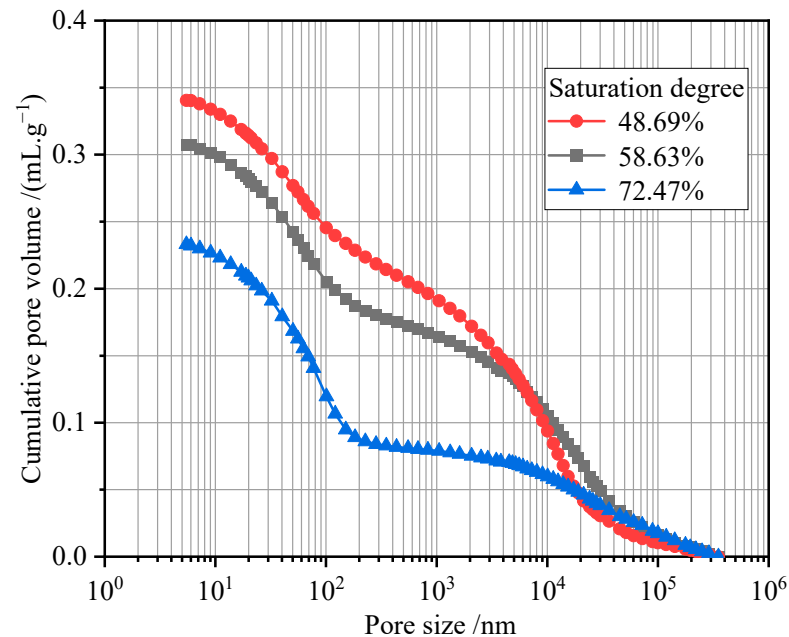


Figure 18. Pore size distribution curves under different saturation degrees.

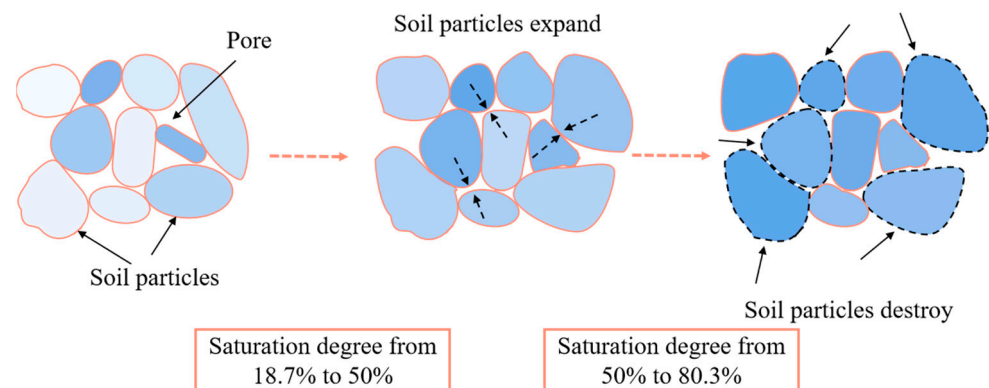


Figure 19. Mechanisms of soil particles and pore changes.

4.3. Mechanistic Analysis of Changes in Shear Strength of Specimens

Due to the shear strength parameters reflecting the property of shear strength, this paper analyzes the change mechanism of shear strength parameters.

This cohesive force mainly includes the original cohesive force formed by molecular gravity among soil particles, the capillary cohesive force generated by capillary pressure, and the curing cohesive force formed by the cementation of compounds in soils. Therefore, the main reasons for cohesive force changes are as follows: (1) According to the analysis of the uniaxial tensile strength mechanism, the capillary pressure first increased and then decreased when the saturation degree increased from 18.7% to 80.3%. However, the existence of capillary pressure will increase the capillary cohesive force [49]. (2) The hydrophilic mineral composition in expansive soils produces cementation with water [51].

Therefore, there is a curing cohesive force in the soils. According to the analysis of the content change in colloids, the cementation will first increase and then decrease with the increase in saturation degree (see Section 4.1). In summary, due to the influence of capillary cohesive force and curing cohesive force, the cohesive force of specimens will first increase and then decrease with the increase in the saturation degree (see Figure 14a).

The internal friction angle depends on the friction between soil particles and the bite force generated by the chain effect, and the internal friction angle reflects the friction properties of soil. Friction refers to the force that hinders the relative movement of soil particles, and the bite force refers to the force needed to pull out the soil particles embedded between other particles when the soil slides. Therefore, there are two main reasons for the change in internal friction angle. (1) According to the mechanism analysis of cohesive force change, the cohesive force of the specimens first increased and then decreased as the saturation degree increased. However, cohesive force restricted the relative motion of the soil particles. (2) Colloids produced by the hydration of expansive soils will adsorb soil particles. When the saturation degree was between 18.7% and 80.3%, the colloid content of specimens also first increased and then decreased. However, the sliding of the soil particles needed to overcome the bite force generated by this part of the colloids. In summary, with the increase in saturation degree, the internal friction angle will go through two stages. In the first stage (the saturation degree increased from 18.7% to 50%), the internal friction angle of the specimens gradually increased. In the second stage (the saturation degree increased from 50% to 80.3%), the internal friction angle of the specimens gradually decreased (see Figure 14b).

5. Conclusions

In this paper, the effect of saturation degree on the mechanical behaviors of shallow unsaturated expansive soils was studied using a uniaxial tensile test, unconfined compression test, and direct shear test, and the change mechanism for the mechanical behaviors of shallow unsaturated expansive soils was analyzed. The main conclusions are summarized as follows:

- (1) The uniaxial tensile strength, unconfined compressive strength, cohesive force, and internal friction angle of the expansive soils first increased and then decreased with the increase in saturation degree.
- (2) When the saturation degree increased from 18.7% to 57.1%, the uniaxial tensile strength increased by about 11 times. When the saturation degree increased from 57.1% to 80.3%, it decreased by about 42%.
- (3) The saturation degrees from 18.7% to 50%, the unconfined compressive strength, cohesive force, and internal friction angle increased by about 3.24 times, 2.34 times, and 0.52 times, respectively. The saturation degrees from 50% to 80.3% decreased by about 51.4%, 36%, and 50%, respectively.
- (4) The change in hydrophilic mineral composition and pore structure is one of the important reasons for the mechanical behavior change in expansive soils.

Author Contributions: Conceptualization, J.L., B.L. and D.L.; data curation, B.L., S.R. and J.W.; formal analysis, L.C.; funding acquisition, H.X., L.C. and D.L.; investigation, H.X.; methodology, H.X.; supervision, L.C.; writing—original draft, J.L. and S.Z.; writing—review and editing, J.L. All authors have read and agreed to the published version of the manuscript.

Funding: The authors are grateful to the financial support from the National Key Research and Development Program of China (2021YFB3901403), the Special Project for Performance Incentive and Guidance of Scientific Research Institutions in Chongqing (cstc2021jxjl120011), and the National Natural Science Foundation of China (52027814).

Institutional Review Board Statement: Not applicable.

Informed Consent Statement: Not applicable.

Data Availability Statement: Not applicable.

Conflicts of Interest: The authors declare that they have no known competing financial interests or personal relationships that could have appeared to influence the work reported in this paper.

References

1. Gullà, G.; Mandaglio, M.C.; Moraci, N. Effect of weathering on the compressibility and shear strength of a natural clay. *Can. Geotech. J.* **2006**, *43*, 618–625. [[CrossRef](#)]
2. Zhao, Y. Transient stability analysis method and sensitivity study of unsaturated soil slopes under consideration of rainfall conditions. *Arab. J. Geosci.* **2021**, *14*, 1179. [[CrossRef](#)]
3. Xu, W.H.; Kang, Y.F.; Chen, L.C.; Wang, L.Q.; Qin, C.B.; Zhang, L.T.; Liang, D.; Wu, C.Z.; Zhang, W.G. Dynamic assessment of slope stability based on multi-source monitoring data and ensemble learning approaches: A case study of Jiuxianping landslide. *Geol. J.* **2022**, 1–19. [[CrossRef](#)]
4. Hou, T.S.; Xu, G.L.; Shen, Y.J.; Wu, Z.Z.; Zhang, N.N.; Wang, R. Formation mechanism and stability analysis of the Houba expansive soil landslide. *Eng. Geol.* **2013**, *161*, 34–43. [[CrossRef](#)]
5. Zhang, J.R.; Niu, G.; Li, X.C.; Sun, D.A. Hydro-mechanical behavior of expansive soils with different dry densities over a wide suction range. *Acta Geotech.* **2020**, *15*, 265–278. [[CrossRef](#)]
6. Xiao, J.; Yang, H.P.; Zhang, J.H.; Tang, X.Y. Properties of Drained Shear Strength of Expansive Soil Considering Low Stresses and Its Influencing Factors. *Int. J. Civ. Eng.* **2018**, *16*, 1389–1398. [[CrossRef](#)]
7. Cokca, E.; Erol, O.; Armangil, F. Effects of compaction moisture content on the shear strength of an unsaturated clay. *Geotech. Geol. Eng.* **2004**, *22*, 285–297. [[CrossRef](#)]
8. Vanapalli, S.K.; Fredlund, D.G.; Pufahl, D.E.; Clifton, A.W. Model for the prediction of shear strength with respect to soil suction. *Can. Geotech. J.* **1996**, *33*, 379–392. [[CrossRef](#)]
9. Çokça, E.; Tilgen, H.P. Shear strength-suction relationship of compacted Ankara clay. *Appl. Clay Sci.* **2010**, *49*, 400–404. [[CrossRef](#)]
10. Abeykoon, T.; Trofimovs, J. Shear strength of unsaturated expansive soils from queensland natural slopes. *Int. J. GEOMATE* **2021**, *20*, 53–60. [[CrossRef](#)]
11. Liu, K.; Ye, W.J.; Jing, H.J. Shear strength and damage characteristics of compacted expansive soil subjected to wet–dry cycles: A multi-scale study. *Arab. J. Geosci.* **2021**, *14*, 2866. [[CrossRef](#)]
12. Duan, M.; Jiang, C.B.; Yin, W.M.; Yang, K.; Li, J.Z.; Liu, Q.J. Experimental study on mechanical and damage characteristics of coalunder true triaxial cyclic disturbance. *Eng. Geol.* **2021**, *295*, 106445. [[CrossRef](#)]
13. Miao, L.C.; Liu, S.Y.; Lai, Y.M. Research of soil-water characteristics and shear strength features of Nanyang expansive soil. *Eng. Geol.* **2002**, *65*, 261–267. [[CrossRef](#)]
14. Yavari, N.; Tang, A.M.; Pereira, J.M.; Hassen, G. Effect of temperature on the shear strength of soils and the soil-structure interface. *Can. Geotech. J.* **2016**, *53*, 1186–1194. [[CrossRef](#)]
15. Tang, L.; Cong, S.Y.; Geng, L.; Liang, X.Z.; Gan, F. The effect of freeze-thaw cycling on the mechanical properties of expansive soils. *Cold Reg. Sci. Technol.* **2018**, *145*, 197–207. [[CrossRef](#)]
16. Elkady, T.Y.; Al-Mahbashi, A.M. Effect of solute concentration on the volume change and shear strength of compacted natural expansive clay. *Environ. Earth Sci.* **2017**, *76*, 483. [[CrossRef](#)]
17. Hajjat, J.; Al-Jeznawi, D.; Sánchez, M.; Avila, G. Effects of Drying and Soil-Base Interface on the Behavior of an Expansive Soil Mixture. *Geotech. Geol. Eng.* **2020**, *38*, 4637–4649. [[CrossRef](#)]
18. Liu, Y.B.; Lebedev, M.; Zhang, Y.H.; Wang, E.Y.; Li, W.P.; Liang, J.B.; Feng, R.H.; Ma, R.P. Micro-Cleat and Permeability Evolution of Anisotropic Coal During Directional CO₂ Flooding: An In Situ Micro-CT Study. *Nat. Resour. Res.* **2022**, *31*, 2805–2818. [[CrossRef](#)]
19. Huang, Z.; Wei, B.X.; Zhang, L.J.; Chen, W.; Peng, Z.M. Surface Crack Development Rules and Shear Strength of Compacted Expansive Soil Due to Dry-Wet Cycles. *Geotech. Geol. Eng.* **2019**, *37*, 2647–2657. [[CrossRef](#)]
20. Zhai, Q.; Rahardjo, H.; Satyanaga, A.; Dai, G.L. Estimation of unsaturated shear strength from soil-water characteristic curve. *Acta Geotech.* **2019**, *14*, 1977–19904. [[CrossRef](#)]
21. Zhai, Q.; Dai, G.L.; Zhao, X.L. Effect of soil-water characteristic curve on shear strength of unsaturated sandy soils. *Chin. J. Geotech. Eng.* **2020**, *42*, 1341–1349. (In Chinese) [[CrossRef](#)]
22. Phanikumar, B.R.; Raju, E.R. Compaction and strength characteristics of an expansive clay stabilised with lime sludge and cement. *Soils Found.* **2020**, *60*, 129–138. [[CrossRef](#)]
23. Chenarboni, H.A.; Lajevardi, S.H.; MolaAbasi, H.; Zeighami, E. The effect of zeolite and cement stabilization on the mechanical behavior of expansive soils. *Constr. Build. Mater.* **2021**, *272*, 121630. [[CrossRef](#)]
24. Jain, A.K.; Jha, A.K.; Shivanshi. Geotechnical behaviour and micro-analyses of expansive soil amended with marble dust. *Soils Found.* **2020**, *60*, 737–751. [[CrossRef](#)]
25. Singh, P.; Dash, H.K.; Samantaray, S. Effect of silica fume on engineering properties of expansive soil. *Mater. Today Proc.* **2020**, *33*, 5035–5040. [[CrossRef](#)]
26. Kang, Y.F.; Fan, J.Y.; Jiang, D.Y.; Li, Z.Z. Influence of Geological and Environmental Factors on the Reconsolidation Behavior of Fine Granular Salt. *Nat. Resour. Res.* **2021**, *30*, 805–826. [[CrossRef](#)]
27. Ding, L.Q.; Vanapalli, S.K.; Zou, W.L.; Han, Z.; Wang, X.Q. Freeze-thaw and wetting-drying effects on the hydromechanical behavior of a stabilized expansive soil. *Constr. Build. Mater.* **2021**, *275*, 122162. [[CrossRef](#)]

28. Kushwaha, S.S.; Kishan, D.; Dindorkar, N. Stabilization of expansive soil using eko soil enzyme for Highway Embankment. *Mater. Today Proc.* **2018**, *5*, 19667–19679. [[CrossRef](#)]
29. Divya, V.; Asha, M.N. Performance Evaluation of Bio-Stabilized Soils in Pavements. *Recent Trends Civ. Eng.* **2021**, *77*, 523–529. [[CrossRef](#)]
30. Agarwal, P.; Kaur, S. Effect of Bio-enzyme stabilization on unconfined compressive strength of expansive soil. *Int. J. Res. Eng. Technol.* **2014**, *3*, 30–33.
31. Patel, U.; Singh, S.; Chaudhari, S. Effect of Bio-enzyme TerraZyme on Compaction, Consistency Limits and Strength Characteristics of Expansive Soil. *Int. Res. J. Eng. Technol.* **2015**, *5*, 1602–1605.
32. Soltani, A.; Deng, A.; Taheri, A.; Mirzababaei, M. A sulphonated oil for stabilisation of expansive soils. *Int. J. Pavement Eng.* **2019**, *20*, 1285–1298. [[CrossRef](#)]
33. Liu, Q.B.; Xiang, W.; Zhang, W.F.; Cui, D.S. Experimental study on the modification of swelling soil by ionic soil curing agent. *Rock Soil Mech.* **2009**, *30*, 2286–2290. (In Chinese) [[CrossRef](#)]
34. Rabab'ah, S.; Ai Hattamleh, O.; Aldeeky, H.; Alfoul, B.A. Effect of glass fiber on the properties of expansive soil and its utilization as subgrade reinforcement in pavement applications. *Case Stud. Constr. Mater.* **2021**, *14*, e00485. [[CrossRef](#)]
35. Hasan, H.; Dang, L.; Khabbaz, H.; Fatahi, B.; Terzaghi, S. Remediation of Expansive Soils Using Agricultural Waste Bagasse Ash. *Procedia Eng.* **2016**, *143*, 1368–1375. [[CrossRef](#)]
36. Soğancı, A.S. The Effect of Polypropylene Fiber in the Stabilization of Expansive Soils. *Int. J. Geol. Environ. Eng.* **2015**, *104*, 994–997. [[CrossRef](#)]
37. Bekhiti, M.; Trouzine, H.; Rabehi, M. Influence of waste tire rubber fibers on swelling behavior, unconfined compressive strength and ductility of cement stabilized bentonite clay soil. *Constr. Build. Mater.* **2019**, *208*, 304–314. [[CrossRef](#)]
38. Nitin, T.; Neelima, S.; Anand, J.P. Strength and durability assessment of expansive soil stabilized with recycled ash and natural fibers. *Transp. Geotech.* **2021**, *29*, 100556. [[CrossRef](#)]
39. Arvind, K.; Baljit, S.W.; Asheet, B. Influence of Fly Ash, Lime, and Polyester Fibers on Compaction and Strength Properties of Expansive Soil. *J. Mater. Civ. Eng.* **2007**, *19*, 242–248. [[CrossRef](#)]
40. Nitin, T.; Neelima, S.; Meghna, S. Micro-mechanical performance evaluation of expansive soil biotreated with indigenous bacteria using MICP method. *Sci. Rep.* **2021**, *11*, 10324. [[CrossRef](#)]
41. Sun, D.A.; Matsuoka, H.; Xu, Y.F. Collapse Behavior of Compacted Clays in Suction-Controlled Triaxial Tests. *Geotech. Test. J.* **2004**, *27*, 362–370. [[CrossRef](#)]
42. Sun, D.A.; Matsuoka, H.; Cui, H.B.; Xu, Y.F. Three-dimensional elasto-plastic model for unsaturated compacted soils with different initial densities. *Int. J. Numer. Anal. Methods Geomech.* **2003**, *27*, 1079–1098. [[CrossRef](#)]
43. Sun, D.A.; Sheng, D.C.; Cui, H.B.; Sloan, S.W. A density-dependent elastoplastic hydro-mechanical model for unsaturated compacted soils. *Int. J. Numer. Anal. Methods Geomech.* **2007**, *31*, 1257–1279. [[CrossRef](#)]
44. Zhai, Q.; Rahardjo, H.; Satyanaga, A.; Dai, G.L. Estimation of tensile strength of sandy soil from soil–water characteristic curve. *Acta Geotech.* **2020**, *15*, 3371–3381. [[CrossRef](#)]
45. Wang, X.; Cui, J.; Wu, Y.; Zhu, C.Q.; Wang, X.Z. Mechanical properties of calcareous silts in a hydraulic fill island-reef. *Mar. Georesources Geotechnol.* **2020**, *39*, 1–14. [[CrossRef](#)]
46. Zhai, Q.; Rahardjo, H.; Satyanaga, A.; Dai, G.L.; Zhuang, Y. Framework to estimate the soil-water characteristic curve for soils with different void ratios. *Bull. Eng. Geol. Environ.* **2020**, *79*, 4399–4409. [[CrossRef](#)]
47. Wu, Y.; Wang, X.; Shen, J.H.; Cui, J.; Zhu, C.Q.; Wang, X.Z. Experimental Study on the Impact of Water Content on the Strength Parameters of Coral Gravelly Sand. *J. Mar. Sci. Eng.* **2020**, *8*, 634. [[CrossRef](#)]
48. Wu, Y.; Cui, J.; Li, N.; Wang, X.; Wu, Y.H.; Guo, S.Y. Experimental study on the mechanical behavior and particle breakage characteristics of hydraulic filled coral sand on a coral reef island in the South China Sea. *Rock Soil Mech.* **2020**, *41*, 3181. [[CrossRef](#)]
49. Hassanizadeh, S.M.; Celia, M.A.; Dahle, H.K. Dynamic effect in the capillary pressure–saturation relationship and its impacts on unsaturated flow. *Vadose Zone J.* **2002**, *1*, 38–57. [[CrossRef](#)]
50. Li, J.; Wu, X.Y.; Hou, L. Physical, Mineralogical, and Micromorphological Properties of Expansive Soil Treated at Different Temperature. *J. Nanomater.* **2014**, *2014*. [[CrossRef](#)]
51. Yu, X.P.; Xiao, H.B.; Li, Z.Y.; Qian, J.F.; Luo, S.P.; Su, H. Experimental Study on Microstructure of Unsaturated Expansive Soil Improved by MICP Method. *Appl. Sci.* **2022**, *12*, 2076–3417. [[CrossRef](#)]
52. Chang, J.; Yang, H.P.; Xiao, J.; Xu, Y.F. Soil-water chemical tests and action mechanism of acid rain infiltration into expansive soil. *Chin. J. Geotech. Eng.* **2022**, *44*, 1483–1492. (In Chinese) [[CrossRef](#)]
53. Li, Y.Z.; Wang, S.M.; Zou, J.W.; Wang, H.; Li, H.; Wu, N. Correlation Research between Shear Strength and Moisture Content of Swelling Mudstone. *Sci. Technol. Eng.* **2021**, *21*, 2857–2864. (In Chinese)
54. Wei, J.; Shi, B.L.; Li, J.L.; Li, S.S.; He, X.B. Shear strength of purple soil bunds under different soil water contents and dry densities: A case study in the Three Gorges Reservoir Area, China. *CATENA* **2018**, *166*, 124–133. [[CrossRef](#)]
55. Dai, Z.J.; Chen, S.X.; Li, J. Physical model test of seepage and deformation characteristics of shallow expansive soil slope. *Bull. Eng. Geol. Environ.* **2020**, *79*, 4063–4078. [[CrossRef](#)]